The final publication is available at

http://dx.doi.org/10.1016/j.seppur.2015.07.051

Additional Information

Selective recovery of zinc from spent pickling baths by the combination of membrane-based solvent extraction and electrowinning technologies

Jordi Carrillo-Abad[a], Montserrat Garcia-Gabaldon[a]*, Isabel Ortiz-Gandara[b], Eugenio Bringas[b], Ane Miren Urtiaga[b], Inmaculada Ortiz[b], Valentin Perez-Herranz[a].

[a] *Departamento de Ingeniería Química y Nuclear, Universidad Politécnica de Valencia, P.O. Box 22012, E-46023 Valencia, España.*

[b] *Departamento de Ingenierías Química y Biomolecular, Universidad de Cantabria, 39005, Santander, España.*

*Correspondence to: Departamento de Ingeniería Química y Nuclear, Universidad Politécnica de Valencia, P.O. Box 22012, E-46023 Valencia, España.

E-mail: mongarga@iqn.upv.es; Phone: +34 963877007 ext. 76313; Fax: +34 963879632

ABSTRACT

This work deals with the analysis of an integrated zinc recovery process by means of electrowinning of the stripping solutions coming from the treatment of spent pickling baths (SPB) by a membrane–based solvent extraction (MBSX) process able of increasing the initial Zn/Fe molar ratio. Several stripping solutions containing different concentrations of zinc and iron in acid media obtained previously by the treatment of SPB by MBSX, were subjected to electrowinning to assess the efficiency and selectivity of zinc electrodeposition over iron under different operation conditions.

At similar values of the zinc concentration in the stripping solution, the influence of the Zn/Fe molar ratio on the zinc electrodeposition process was negligible. On the other hand, although the variation of the initial concentration of zinc in the stripping solution neither affected the efficiency of zinc electrowinning, it increased the minimum value of zinc concentration in solution beyond which iron co-deposition started. Finally, the increase in the applied current, promoted the increase in zinc fractional conversion and in the zinc space-time yield, while the zinc current efficiency was reduced due to the stronger effect of secondary reactions.

Although the change in the stripping characteristics seems not to strongly affect the zinc electrodeposition process, the use of a pretreatment step based on MBSX technology improved the results in terms of zinc percentage recovered and the rest of figures of merit, in comparison with those obtained by the direct electrowinning of SPB.

Keywords: Electrowinning, iron, membrane-based solved extraction, spent-pickling baths, zinc.

1. INTRODUCTION

The hot dip galvanizing process, which consists on the dipping of steel pieces in molten zinc in order to protect them from corrosion [1], generates a succession of effluents among which it is worth to note the spent pickling baths (SPB) as the highest polluting effluent. The SPB, whose purpose is to clean the pieces surface from rust and impurities by its attack with HCl, contains high concentrations of $ZnCl_2$, $FeCl_2$ in HCl media [2] and, consequently, they have to be treated previous to their disposal. However, the traditional treatment process, which consists in the effluent neutralization and the precipitation of the iron and zinc as hydroxides, presents as disadvantages the high consumption of chemical products together with the generation of a hazardous sludge that has to be treated [3]. In addition, the decrease of natural reserves of non-ferrous metals makes zinc recovery an interesting alternative of treatment.

In our previous works [4-8], zinc recovery from SPB by means of an electrochemical membrane reactor, which avoids the redissolution of the zinc deposits by the attack of the chlorine generated in the anode, has been successfully applied in order to obtain metallic zinc that can be directly reintroduced into the galvanizing process. However, the anomalous codeposition among zinc and iron [9, 10] avoids the possibility of recovering all the zinc present in the SPB without iron presence in the deposit.

On the other hand, different membrane-based solvent extraction (MBSX) process configurations namely Emulsion Pertraction Technology (EPT) and Non-Dispersive Solvent Extraction (NDSX), which differ in the way of contacting the fluid phases and the number of the membrane contactors involved, have proved to be efficient alternatives to perform the selective separation of zinc over iron in HCl media employing tributylphosphate (TBP) and water as extraction and stripping agents, respectively [11-14]. In a previous work [14], the effect of several process variables on

the kinetics and selectivity of zinc over iron separation was analyzed in order to obtain a highly concentrated zinc solution with a negligible content of iron to allow for further recovery of zinc by electrowinning. It was concluded that the kinetics of extraction and stripping of zinc and iron were promoted by EPT configuration in comparison with NDSX configuration, and increasing the TBP concentration in the range between 20% (v/v) and 50% (v/v). Therefore, a suitable selection of the optimal operation conditions is required to maximize the molar ratio zinc/iron in the stripping solution.

In this sense, this work is the combination of electrowinning and membrane-based solvent extraction technologies in order to create a hybrid process to maximize both the yield and selectivity of zinc recovery from spent pickling baths. More specifically, this work analyses the efficiency and selectivity of zinc electrodeposition from stripping solutions containing different concentrations of zinc and iron which were previously obtained by the treatment of SPB by EPT under different operation conditions. In addition, other parameters such as the influence of the applied current in the electrowinning process are also evaluated.

2. MATERIALS AND METHODS

2.1 Membrane-based solvent extraction experiments

The experiments were performed at laboratory scale using one mesoporous hollow fiber membrane contactor (HFMC, Liqui-Cel® Extra-Flow 2.5x8, Hoechst Celanese) containing 10200 polypropylene fibers with an effective mass-transfer area of 1.4 m^2 and an effective mass-transfer length of 0.15 m. The fibers had a nominal porosity of 40%, an average pore size of 0.03 μm and an internal diameter of 240 μm with a wall thickness of 30 μm. Figure 1 shows the experimental set-up used for the extraction and

back-extraction of zinc from the aqueous systems using the Emulsion Pertraction Process configuration. In EPT configuration the extraction and back extraction of the target species were conducted in a single membrane module and the non-dispersive contact occurred between the feed SPB and the pseudo-emulsion prepared by dispersing the stripping solution into the organic phase. The difference in the transmembrane pressure between the aqueous phase and the emulsion phase was maintained constant at approximately 0.15 bars in order to avoid the dispersion of the organic fluid into the feed aqueous phases. The organic and the stripping phases can be easily separated by gravity settling. Further details of the experimental procedure are found elsewhere [15, 16].

The feed solutions consist of 500 mL of SPB provided by a local industry and containing mainly zinc, iron, chloride and free acid (Table 1). The organic solution was formulated by dilution of the extractant TBP (97%, Sigma-Aldrich) in the aliphatic solvent Shellsol D70 (Kremer Pigmente). Tap water was utilised as stripping solution in all the experiments. The pseudo-emulsion was formulated by dispersing 200 mL of the stripping solution into 800 mL of the organic phase using a stirrer MRVS-08 (SBS).

Due to the dependence of zinc and iron extraction and back-extraction kinetics on the operation conditions [14] and with the aim of attaining stripping solutions with different concentrations of zinc and iron, EPT experiments were performed under different operation conditions namely the operation time in the range between 1 and 3 hours and the concentration of the selective extractant TBP varying from 20% (v/v) and 50% (v/v). Table 2 summarizes the conditions of EPT and electrowinning (EW) experiments, and the pH and composition of the stripping solutions employed in electrolysis experiments.

Zinc and iron determination was performed by atomic absorption spectrophotometry (AAS). The determination of zinc was performed on a Perkin–Elmer model Analyst 100 atomic absorption spectrophotometer using a zinc hollow cathode lamp at 213.9 nm wavelength, 0.7 nm spectral bandwidth and an operating current of 5 mA. The iron concentration was performed using the same equipment with a Fe hollow lamp; the wavelength selected was 248.3 nm, the applied operating current was 5 mA and the spectral bandwidth was 0.2 nm [4-8].

2.2 Electrowinning experiments

The electrowinning (EW) experiments were performed in a membrane reactor. Although this reactor is well defined in our previous works [4-8], its schematic representation is shown in Figure 2, which also includes the main reactions for both electrodes. The membrane reactor is filled, after the cell assembly, with an equal volume of 250 cm^3 of catholyte and anolyte in their respective compartments. A graphite cathode, titanium anode and Ag/AgCl reference electrode were employed in this reactor. Both cathode and anode were completely immersed in the solutions and symmetrically placed. The cathode consisted of 4 cylindrical graphite bars with an effective area of 28.30 cm^2 whereas the anode is made of a titanium mail.

The membrane used in the reactor was an IONICS AR-204-SZRA-412 anion-exchange membrane (AEM) which was placed between both compartments. Moreover, in this reactor the catholyte was formulated with the stripping solutions obtained by the treatment of SPB by EPT, whereas the anolyte consisted of a 0.1M HCl synthetic solution prepared from analytical grade reagents and distilled water. All experiments were performed at room temperature.

Experiments were conducted at different applied currents, which ranged from −700 mA to −1500 mA. The equipment used for the electrolysis experiments was an Autolab PGSTAT20 potentiostat/galvanostat. Potential, cell voltage, current, pH and temperature were recorded during the electrowinning. Samples of 1 ml were taken from the reactor every 30 min in order to quantify zinc and iron concentrations as described above.

Table 2 compiles the selected conditions for EW experiments which are grouped in three different categories with the aim of analysing the influence on the efficiency and selectivity of zinc electrodeposition of the following operation variables: i) the initial Zn/Fe molar ratio keeping constant the initial concentration of zinc (experiments 5-8), ii) the initial concentration of zinc (experiments 1-4), and iii) the applied current employing solutions with similar characteristics (experiments 8-10). In order to facilitate the analysis, stripping solutions were doped with Fe^{2+}, employing $FeCl_2$ (98% Sigma-Aldrich), in experiments 5-7.

3. RESULTS AND DISCUSSION

In this section the effect on zinc electrodeposition of several operation parameters influencing the efficiency of the electrochemical process is analyzed in order to select the most favourable conditions to maximize the yield and selectivity of zinc recovery. In this sense, the zinc and iron concentrations, together with another parameters were followed and recorded during the electrolysis to calculate the corresponding figures of merit [17, 18]. Firstly, the zinc and iron removal rates are determined using Eq. (1):

$$X(t) = \frac{C_0 - C(t)}{C_0}$$

(1)

where C_0 (M) is the initial concentration of zinc or iron present in the solution and $C(t)$ (M) corresponds to the concentration of these species at a given time. Moreover, the current efficiency, which relates the current used to deposit zinc with the total current input is an indicative of the efficiency of the zinc deposition process and was calculated by Eq. (2) [19]:

$$\phi(t)(\%) = \frac{n \cdot F \cdot (C_0 - C(t)) \cdot V}{\int_0^t I(t) \cdot dt} \cdot 100 \tag{2}$$

where n is the number of electrons exchanged in the metal deposition, F is the Faraday's constant, V (l) is the reactor volume and $I(t)$ (A) is the applied current at a certain instant of time (h). On the other hand, the space-time yield, $\eta(t)$ ($g \cdot l^{-1} \cdot h^{-1}$) is a parameter associated with the achieved productivity that indicates the mass of zinc deposited per unit of volume and time and is defined by Eq. (3):

$$\eta(t) = \frac{M \cdot (C_0 - C(t))}{t} \tag{3}$$

where M is the atomic weight of zinc ($g \ mol^{-1}$) and t (h) is a given instant time. Finally, the specific energy consumption, $E_s(t)$ ($kW \ h \ kg^{-1}$) which is used to quantify the amount of energy consumed per mass unit of zinc was calculated using the following equation:

$$E_s(t) = \frac{\int_0^t U(t) \cdot I(t) \cdot dt}{V \cdot C_0 \cdot X(t) \cdot M \cdot 3600} \tag{4}$$

where $U(t)$ (V) is the cell potential at a given instant time.

3.1 Effect of the Zn/Fe molar ratio of the stripping solution.

This operation variable was modified according to the typical molar ratios observed in the stripping solutions obtained by the treatment of SPB by MBSX technology [14]. For this purpose different amounts of synthetic iron were added to the stripping solutions being the initial concentration of zinc kept constant as reported in experiments 5-8 present in Table 2. Figure 3 shows the evolution with time of zinc fractional conversion and the mols of zinc deposited on the cathode surface (inset in Figure 3) as a function of the initial Zn/Fe molar ratio of the stripping solution under an applied current of -0.7A. From the results depicted in Figure 3 and under the selected operation conditions, it is concluded that zinc deposition is not significantly affected by the initial Zn/Fe molar ratios studied, being the slight differences between the experimental data attributed to either the experimental error or to the slight variation of the initial concentrations of zinc. Similar conclusions were obtained from experiments performed at similar Zn/Fe molar ratio when the applied current was set at values of -1A and -1.5A (not shown).

Figure 4 represents the time evolution of iron fractional conversion together with the zinc concentration for all the Zn/Fe molar ratios under study. In this case, the zinc concentration beyond which iron begins to co-deposit ranges from 0.06 to 0.1 M, and the iron co-deposition phenomenon starts approximately at the same instant time value, 660 min, independently of the initial amount of iron present in the solution. This fact is associated with the breakup of the $Zn(OH)_2$ film present around the cathode, which inhibits the iron deposition. The reduction of iron in the presence of zinc follows an anomalous co-deposition mechanism where the more noble metal (iron) is not firstly deposited since the zinc present in the solution forms, previously to its deposition, a zinc hydroxide film around the cathode that inhibits the iron deposition as describes the model suggested by *Dahms* [20]. This phenomenon is strongly affected by the pH, applied current, stirring rate and zinc concentration [7,9,10].

Therefore, from the data presented in Figure 3 and 4, it is concluded that under the selected operation conditions, the amount of zinc recovered previously to the iron co-deposition is not affected by the initial iron concentration in the stripping solution. Finally, the other figures of merit present similar values independently of the Zn/Fe molar ratio even the specific energy consumption since the Zn/Fe molar ratio neither affect the cell potential values obtained.

As the recovery of zinc from the stripping solution by electrowinning is not affected by the presence of iron for the initial Zn/Fe molar ratios analysed, the design of a MBSX process for the treatment of SPB could be simplified since the operation conditions should be selected to maximize the extraction and recovery of zinc in the back-extraction solution up to obtain as low Zn/Fe molar ratio as possible.

3.2 Effect of the initial concentration of zinc

Since the amount of zinc deposited under the same applied current and initial zinc concentration was demonstrated not to be affected by the presence of iron, the present section evaluates the influence of the initial zinc concentration on the electrowinning process. As reported in Table 2, several EPT experiments were performed by increasing either the operation time or the TBP concentration in order to obtain stripping solutions with different initial concentrations of zinc in the range from 0.07 to 0.61 M (experiments 1-4). In addition, iron concentration and pH also varied in the ranges of 0.005-0.04 M and 1.67-0.8, respectively due to the unavoidable co-extraction of Fe and H^+ together with zinc species [14] and thus, the values of the initial molar ratio Zn/Fe varied from 14 to 20.

From Figure 5, which shows the evolution with time of the mols of zinc deposited in experiments 1-4 when the applied current is -1A, it is concluded that the change in the initial zinc concentration, practically does not affect the amount of zinc deposited on the cathode surface. This behaviour is explained by the fact that if the applied current remains invariable, the amount of zinc deposited remains constant independently of its initial concentration value, as the current density is proportional to the global reaction velocity.

However, as depicted in Figure 6 the zinc fractional conversion (Eq. 1) is greatly affected by the initial zinc concentration because under the same applied electrical current the zinc deposition rate is constant and thus, the time needed to obtain a 100% zinc fractional conversion grows as the initial zinc concentration increases.

The time evolution of both the iron fractional conversion and the zinc concentration is represented in Figure 7. For experiments 1-3 it is observed that iron co-deposition starts when the zinc concentration diminishes to values amongst 0.01 and 0.02 M independently of the initial zinc and iron concentrations. On the other hand, the zinc concentration measured when the iron co-deposition begins in experiment 4 is almost ten times higher ($\approx$0.12 M) than the observed in experiments 1-3. This may be related with the lesser amount of free zinc present in the stripping solution employed in the performance of experiment 4, as reported in Table 3 [21], where the molar fractions of the zinc chlorocomplexes in the solutions used in experiments 3 and 4 are compiled. Then, the decrease in the free zinc molar fraction, which is related to the higher Cl^-/Zn^{2+} molar ratio, could affect the stability of the $Zn(OH)_2$ layer that inhibits the iron deposition [10] and therefore, the total amount of zinc recovered before iron co-deposition diminishes.

In addition, the bulk solution pH in the cathodic compartment was measured over all the electrolysis time as observed in Figure 8. In all the experiments, the pH in the cathodic compartment increases with time due to the protons consumption related to hydrogen evolution reaction. It is worth to note that a pH value close to 2 is always observed when iron begins to co-deposit with zinc [7,8]. This fact may be associated with the pH effect on the iron deposition observed in our previous works [22], where the inhibition of iron deposition at very low pH values was observed.

3.3 Effect of the applied current.

The effect of the applied current on the zinc fractional conversion, X_{Zn}, for stripping solutions obtained with 50% of TBP during 90 min, which are characterized in Table 2 as experiments 8-10, is shown in Figure 9. It is concluded that the higher the applied current, the higher the zinc fractional conversion since the zinc deposition rate is directly proportional to the applied current.

The iron fractional conversion together with the zinc concentration evolution is represented in Figure 10 for the same experimental conditions as those presented above. As shown in the Figure, an increase in the applied current in absolute value, causes a reduction in the time needed for iron to be co-deposited, which is directly related to the zinc depletion from solution; In all the cases presented, approximately 80% of the zinc is deposited previously to the iron co-deposition.

Figure 11 presents the time evolution of zinc current efficiency as a function of the applied current for the same experimental conditions as those presented previously. For all the applied current values, zinc current efficiency initially reaches higher values but it decreases afterwards due to the zinc depletion from the solution and the consequently

increase in the rate of secondary reactions, such as the hydrogen evolution reaction (HER) and the iron co-deposition. It is worth to note that under these experimental conditions the HER is present from the beginning of the electrolysis and, as a consequence, zinc current efficiency never reaches the 100% value for any applied current. For a given instant time, the higher the applied current is the lower the value of the calculated zinc current efficiency. This is associated with the fact that an increase in the applied current not only improves the zinc deposition rate but also increases the importance of the secondary reactions.

As shown in Figure 12, in general, the space–time yield increases over the initial period because of the nucleation of zinc onto the graphite electrode that causes a decrease in the electrode resistance for the deposition of zinc. Then, the space-time yield decreases as the zinc depletion occurs. It is worth to note that for the lower current value, -0.7A, this parameter remains practically constant during all the electrolysis time, fact which is associated with an applied current lower than the limiting value since the same zinc amount is deposited in each time interval [23]. For a given instant time, the higher the applied current is the higher the space-time yield as a higher applied current implies a higher global reaction rate.

The effect of the applied current on the evolution of the specific energy consumption with time is shown in Figure 13. The general increase of E_s with the applied current can be attributed to the decrease in current efficiency, observed in Figure 11, because of the onset of the HER. For all the applied current values, E_s presents initially lower values as the main reaction is the zinc deposition, but it increases with time as the importance of parallel reactions takes place.

3.4 Comparison among the direct electrowinning of the SPB and the combination of MBSX and electrolysis techniques

Finally, the performance of electrowinning experiments conducted with a 1:10 diluted SPB ($[Zn^{2+}]$=0.218 M; $[Fe^{2+}]$=0.140 M; pH=0.74) and a stripping solution with a similar zinc composition obtained by MBSX (experiment 2 in Table 2) is compared. The results dealing with the time evolution of the zinc fractional conversion depicted in Figure 14 show higher zinc deposition rates when EW is carried out with the previously treated stripping solution. This fact may be related to the change in the main composition of the SPB after their treatment by the MBSX technique, as the chloride reduction or the elimination of other heavy metals present in the SPB, which affects negatively to zinc deposition [24,25], or the elimination of the organic additives used in the SPB [2]. However, the main difference between SPB and the stripping solution is related to the Zn/Fe molar ratio which has values of 1.56 and 20, respectively. The higher iron contain when the SPB has not been previously treated by MBSX techniques could be responsible for the enhancement of the hydrogen evolution reaction that competes directly with zinc for its reduction on the cathode surface, giving as a result the different behaviour of both solutions presented in Figure 14. The HER enhancement in the presence of iron has been previously reported in previous works [6].

Figure 15 shows the evolution of iron fractional conversion together with the zinc concentration for both solutions presented above. In both cases, the zinc concentration beyond which iron starts to co-deposit present a similar value, about 0.025M, since they present a similar initial zinc amount. On the other hand, it is worth to note that although the same current value is applied in both solutions, the time value from which iron co-deposition begins is lower for the pre-treated solution. This fact is associated with the higher zinc deposition rate previously observed for the stripping solution employed in

experiment 2, and consequently, the minimum zinc concentration to break up the zinc hydroxide, allowing the iron co-deposition, is reached before. Regarding the pH evolution, the same behaviour described above is observed for these solutions.

As depicted in Figures 16 and 17, the values of the zinc current efficiency and the zinc space-time yield of the pre-treated solution are higher than those obtained by the electrowinning of the diluted SPB. This fact is associated with the greater zinc deposition rate observed for the pre-treated solution, which means that the secondary reactions are more significant in the SPB as previously mentioned. In both cases, the zinc current efficiency initially shows a maximum value after which, it decreases due to the zinc depletion from solution and the increase in the importance of parallel reactions. In both cases, the zinc space-time yield initially presents higher values due to the nucleation of zinc on the cathode surface, which diminishes the electrode resistance for zinc deposition. Then, this parameter decreases due to the zinc depletion from solution.

On the other hand, the values of E_s (Figure 18) are similar for both experiments. This behaviour is related to the higher cell potential presented in the pre-treated solution, which may be associated with the changes in the solution composition caused by the MBSX treatment (probably the lower iron concentration that decreases the ionic conductivity of the solution).

4. CONCLUSIONS

Stripping solutions with different concentrations of zinc, iron, chloride and free acid obtained by the pre-treatment of spent pickling baths by membrane–based solvent extraction technology under different operation conditions, were treated by electrowinning to analyse the influence on the selectivity of zinc recovery over iron. It is worth to note that in all the experiments carried out, the bulk solution pH measured when iron begins to co-deposit was close to 2, which is related to the inhibition of the iron deposition at high acidic solutions.

Regarding the effect of the initial Zn/Fe ratio under a similar zinc concentration value, no adverse effects on zinc electrowinning were observed as a consequence of increasing iron concentration and thus, the costs related to the pre-treatment of SPB by MBSX may be diminished since a higher iron concentration is allowed in the solutions. On the other hand, the higher the initial zinc concentration, the lower the free zinc amount present in the solution and, consequently, the zinc concentration from which iron begins to co-deposit increases. The effect of the applied current on zinc electrowinning of the stripping solution showed that an increase in the applied current in absolute value produced a reduction in the time needed for iron to be co-deposited. In all the cases approximately 80% of the zinc is deposited previously to the iron co-deposition. Moreover, an increase in the applied current provides a higher zinc recovery but at a higher energy costs.

Finally, the results obtained from the comparison of the electrowinning of a stripping solution with a similar zinc amount to that present in a 1:10 diluted spent pickling bath without previous treatment showed that the pretreatment is beneficial for the zinc electrodeposition process since provides better results in all the figures of merit.

Moreover, although the zinc concentration from which iron begins to co-deposit is similar for both solutions, the time value from which iron co-deposition begins is lower for the pre-treated solution. This fact is associated with the higher zinc deposition rate observed for the pre-treated SPB bath, and consequently, the minimum zinc concentration to break up the zinc hydroxide, allowing the iron co-deposition, is reached before.

REFERENCES

[1] A. R. Marder, The metallurgy of zinc-coated steel, Prog. Mater. Sci. 45 (2000) 191-271.

[2] U. Kerney, Treatment of spent pickling acids from hot dip galvanizing, Resour. Conserv. Recy. 10 (1994) 145–151.

[3] G. Csicsovszki, T. Kékesi, T.I. Török, Selective recovery of Zn and Fe from spent pickling solutions by the combination of anion exchange and membrane electrowinning techniques, Hydrometallurgy 77 (2005) 19–28.

[4] J. Carrillo- Abad, M. García-Gabaldón, E. Ortega, V. Pérez-Herranz, Electrochemical recovery of zinc from the spent pickling baths coming from the hot dip galvanizing industry: Potentiostatic operation, Sep. Purif. Technol. 81 (2011) 200–207.

[5] J. Carrillo-Abad, M. García-Gabaldón, E. Ortega, V. Pérez-Herranz, Recovery of zinc from spent pickling solutions using an electrochemical reactor in presence and absence of an anion-exchange membrane: Galvanostatic operation, Sep. Purif. Technol. 98 (2012) 366-374.

[6] J. Carrillo-Abad, M. García-Gabaldón, V. Pérez-Herranz, Electrochemical recovery of zinc from the spent pickling solutions coming from hot dip galvanizing industries. Galvanostatic operation, Int. J. Electrochem. Sci. 7 (2012) 5442–5456.

[7] J. Carrillo-Abad, M. García-Gabaldón, V. Pérez-Herranz. Treatment of spent pickling baths coming from hot dip galvanizing by means of an electrochemical membrane reactor, Desalination 343 (2014) 38-47.

[8] J. Carrillo-Abad, M. García-Gabaldón, V. Pérez-Herranz. Study of the zinc recovery from spent pickling baths by means of an electrochemical membrane reactor using a cation-exchange membrane under galvanostatic control, Sep. Purif. Technol. 132 (2014) 479-486.

[9] E. Gómez, E. Peláez, E. Vallés, Electrodeposition of zinc + iron alloys: I. Analysis of the initial stages of the anomalous codeposition, J. Electroanal. Chem. 469 (1999) 139–149.

[10] P. Díaz-Arista, O.R. Mattos, O.E. Barcia, F.J. Fabri Miranda, ZnFe anomalous electrodeposition: stationaries and local pH measurements, Electrochim. Acta 47 (2002) 4091–4100.

[11] J. A. Carrera, E. Muñoz, E. Bringas, M.F. San Roman, I. Ortiz, Influence of operation variables on the recovery of zinc from spent pickling effluents using the emulsion pertraction technology, Desalination 245 (2009) 675–679.

[12] J. A. Carrera, E. Bringas, M.F. San Roman, I. Ortiz, Selective membrane alternative to the recovery of zinc from hot-dip galvanizing effluents, J. Membr. Sci. 326 (2009) 672–680.

[13] E. Bringas, M.F. San Roman, A. M. Urtiaga, I. Ortiz, Integrated use of liquid membranes and membrane contactors: Enhancing the efficiency of L-L reactive separations, Chem. Eng. Process.: Process Intensification 67 (2013) 120–129.

[14] J. Laso, V. García, E. Bringas, A. M. Urtiaga, I. Ortiz, Selective Recovery of Zinc over Iron from Spent Pickling Wastes by Different Membrane-based Solvent Extraction Process Configurations, Ind. Eng. Chem. Res. 54 (2015) 3218-3224.

[15] N. Diban, V. García, F. Alguacil, I. Ortiz, A. M. Urtiaga, Temperature enhancement of zinc and iron separation from chromium(III) passivation baths by emulsion pertraction technology, Ind. Eng. Chem. Res. 51 (2012) 9867–9874.

[16] A. M. Urtiaga, E. Bringas, R. Mediavilla, I. Ortiz, The role of liquid membranes in the selective separation and recovery of zinc for the regeneration of Cr(III) passivation baths, J. Membr. Sci. 356 (2010) 88–95.

[17] M. García-Gabaldón, V. Pérez-Herranz, J. García-Antón, J.L. Guiñón, Electrochemical recovery of tin and palladium from the activating solutions of the electroless plating of polymers: Potentiostatic operation, Sep. Purif. Technol. 45 (2005) 183-191.

[18] V. Pérez-Herranz, J. García-Antón, J.L. Guiñón, Ingeniería Electroquímica, Servicio de Publicaciones UPV, Valencia, 1997.

[19] S. Koter, A. Narebska, Current efficiency and transport phenomena in systems with charged membranes, Sep. Sci. Technol. 24 (1989) 1337-1354.

[20] H. Dahms, I. M. Croll, The anomalous codeposition of iron-nickel alloys, J. Electrochem. Soc. 112 (1965) 771-775.

[21] I.Puig-Domenech. Medusa-Chemical Equilibrium Diagrams. (2013).

[22] M. García-Gabaldón, J. Carrillo-Abad, V. Pérez-Herranz, E. M. Ortega-Navarro, Electrochemical study of a simulated spent pickling solution, Int. J. Electrochem. Sci. 6 (2011) 506–519.

[23] F.Coeuret, A.Storck, Eléments de Génie Électrochimique, Lavoisier, Paris, 1984.

[24] M. Karavasteva, The electrodeposition of metal impurities during the zinc electrowinning at high current density in the presence of some surfactants, Hydrometallurgy 35 (1994) 391-396.

[25] L. Muresan, G. Maurin, L. Oniciu, D. Gaga, Influence of metallic impurities on zinc electrowinning from sulphate electrolyte, Hydrometallurgy 43 (1996) 345-354.

Figures and Tables

Fig. 1: EPT experimental setup

Fig. 2. Schematic representation of the membrane reactor.

Fig. 3. Evolution of zinc fractional conversion with time at -0.7A as a function of the initial Zn/Fe molar ratio (experiments 5-8). Inset Fig.: Evolution of zinc moles deposited for the same experimental conditions.

Fig. 4. Evolution of iron fractional conversion (full marks) and zinc concentration (empty marks) with time at -0.7A as a function of the initial Zn/Fe molar ratio (experiments 5-8).

Fig. 5. Evolution of zinc moles deposited with time at -1A in experiments 1-4 performed at different initial concentrations of zinc.

Fig. 6. Evolution of zinc fractional conversion with time at -1A in experiments 1-4 performed at different initial concentrations of zinc.

Fig. 7. Evolution of iron fractional conversion (full marks) and zinc concentration (empty marks) with time at -1A in experiments 1-4 performed at different initial concentrations of zinc.

Fig. 8. Evolution of iron fractional conversion (full marks) and pH (empty marks) with time at -1A in experiments 1-4 performed at different initial concentrations of zinc.

Fig. 9. Evolution of zinc fractional conversion with time as a function of the applied current. Inset Fig.: Evolution of zinc moles deposited for the same experimental conditions.

Fig. 10. Evolution of iron fractional conversion (full marks) and zinc concentration (empty marks) with time as a function of the applied current.

Fig. 11. Evolution of zinc current efficiency with time as a function of the applied current.

Fig. 12. Evolution of zinc space-time yield with time as a function of the applied current.

Fig. 13. Evolution of zinc specific energy consumption with time as a function of the applied current.

Fig. 14. Evolution of zinc fractional conversion with time at -1A for a stripping solution (experiment 2) and a 1:10 diluted spent pickling bath without previous treatment.

Fig. 15. Evolution of iron fractional conversion (full marks) and zinc concentration (empty marks) with time for a stripping solution (experiment 2) and a 1:10 diluted spent pickling bath without previous treatment.

Fig. 16. Evolution of zinc current efficiency with time for a stripping solution (experiment 2) and a 1:10 diluted spent pickling bath without previous treatment.

Fig. 17. Evolution of zinc space-time yield with time for a stripping solution (experiment 2) and a 1:10 diluted spent pickling bath without previous treatment.

Fig. 18. Evolution of zinc specific energy consumption with time for a stripping solution (experiment 2) and a 1:10 diluted spent pickling bath without previous treatment.

Table 1. Composition of real SPB.

Table 2. Experimental conditions of EPT and EW experiments.

Table 3. Initial molar fractions of zinc chlorocomplexes in the stripping solutions employed in EW experiments 3 and 4.
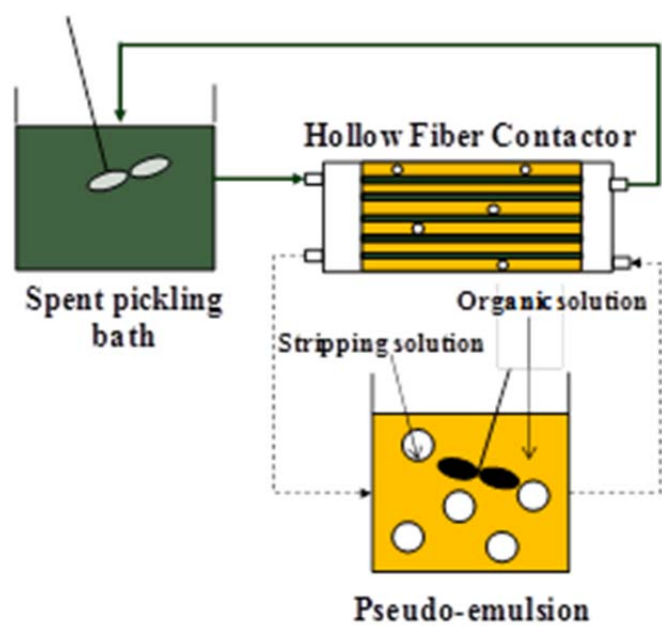
Figure 1
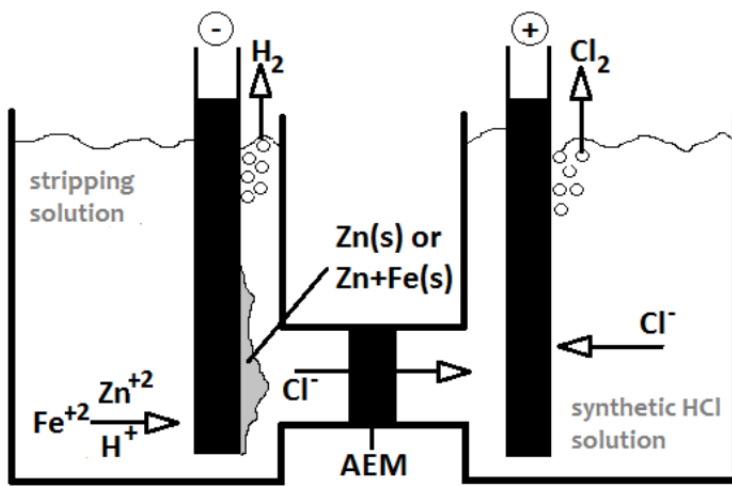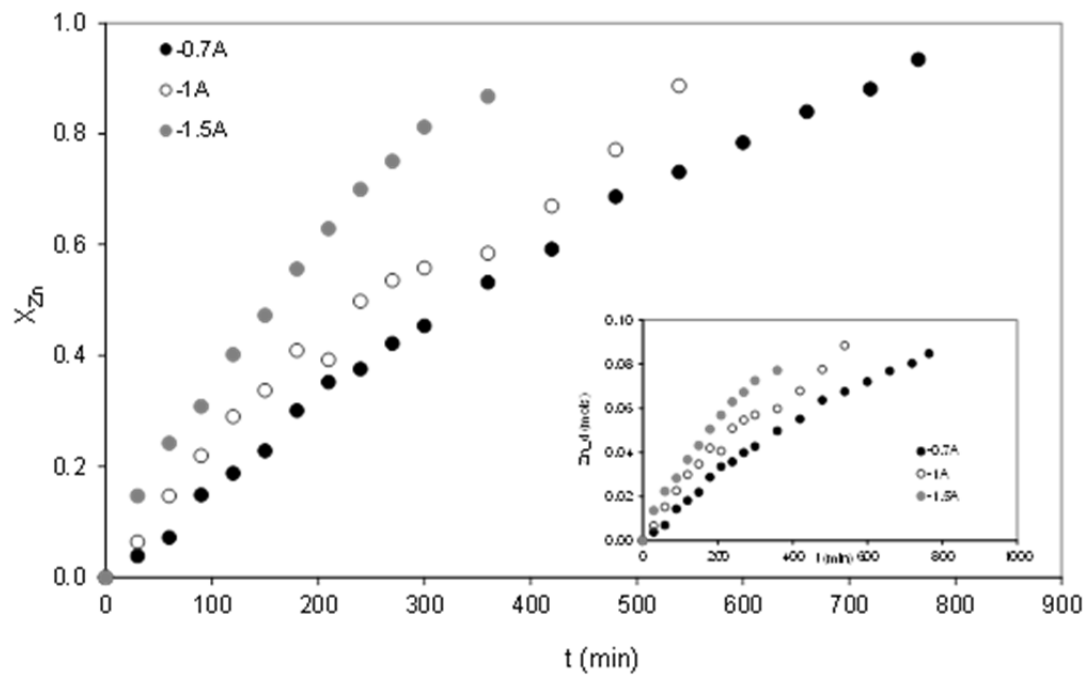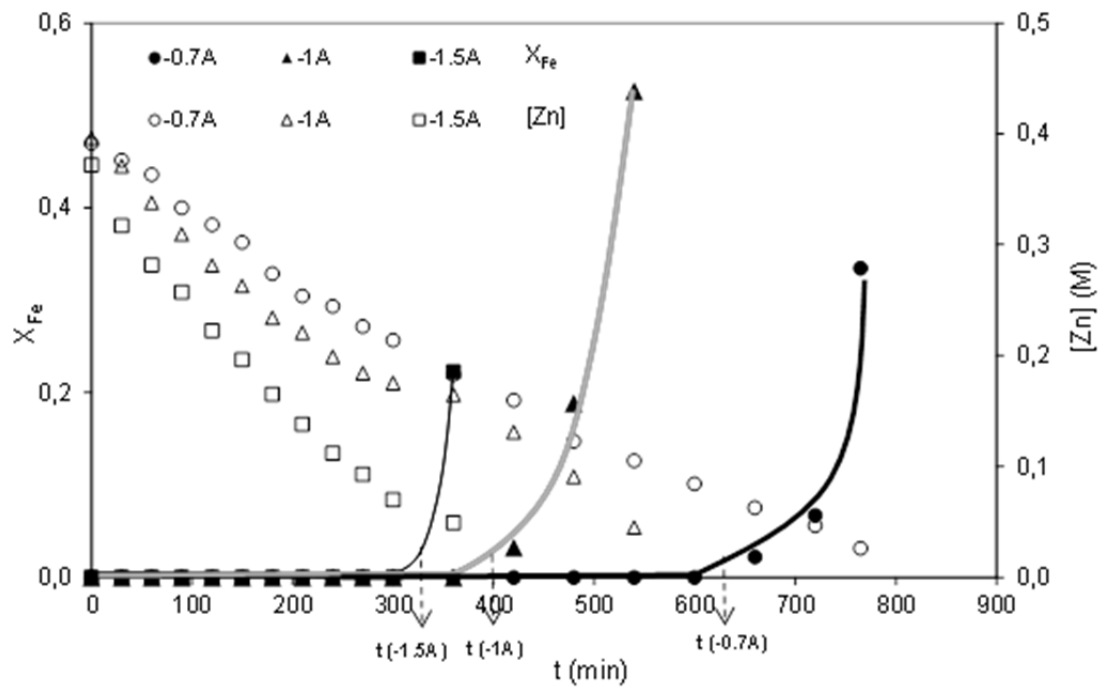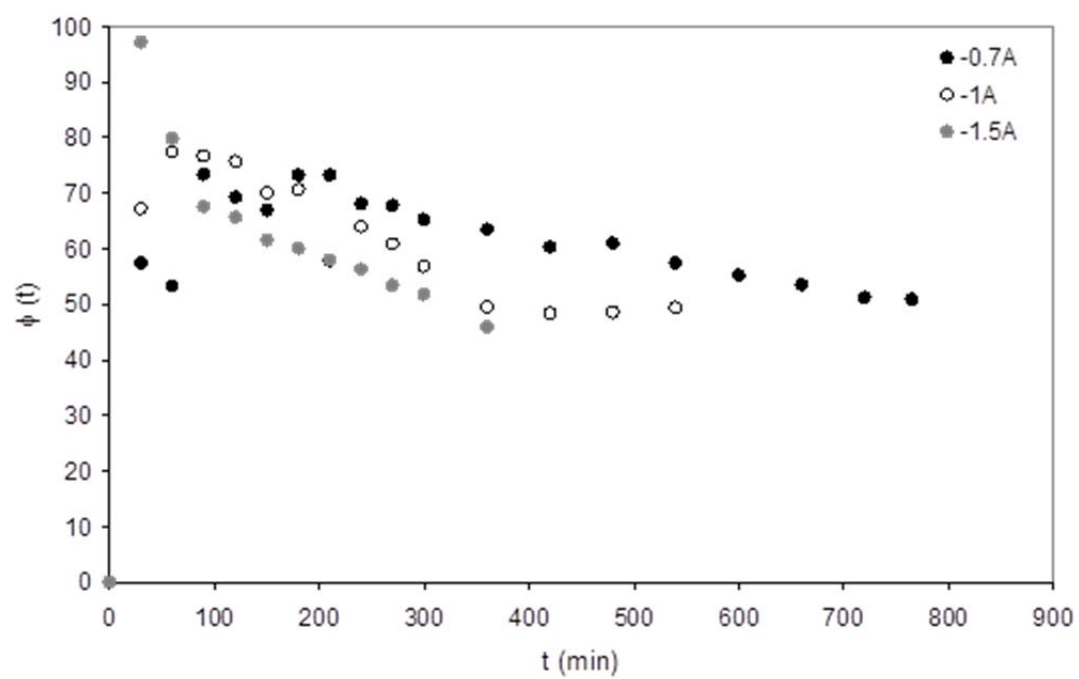
Figure 2
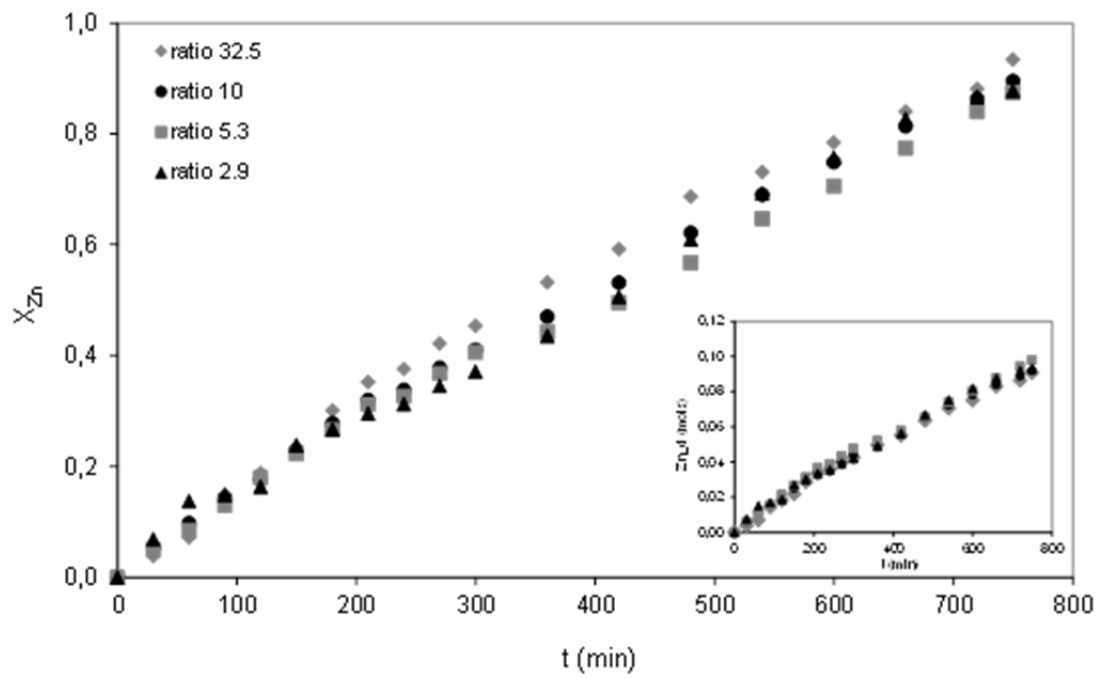
Figure 3
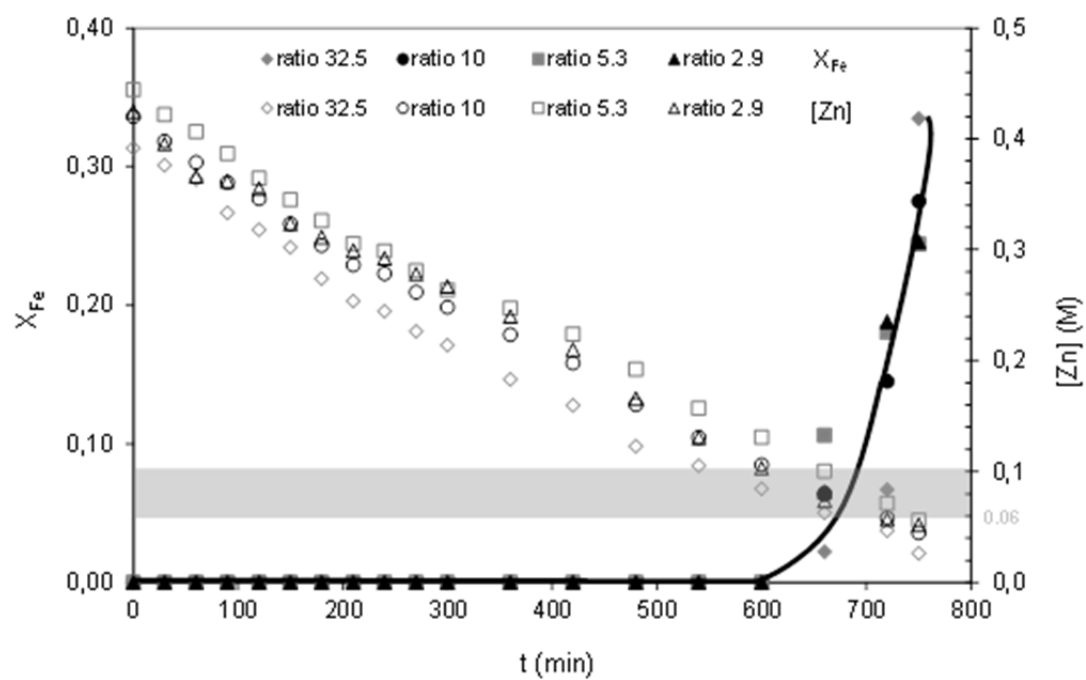
Figure 4
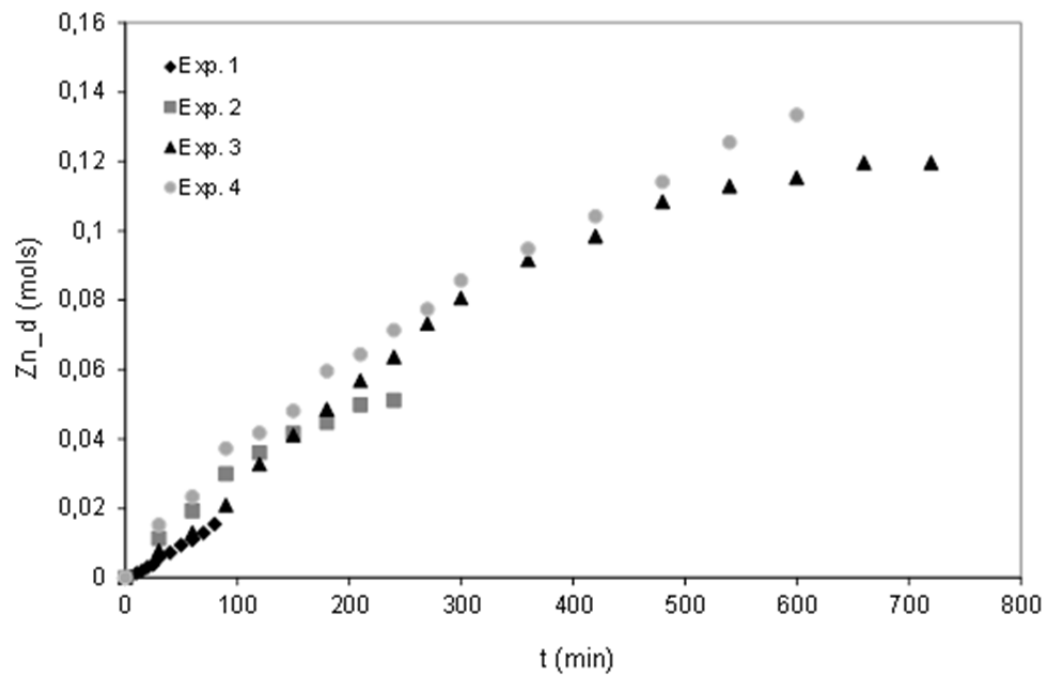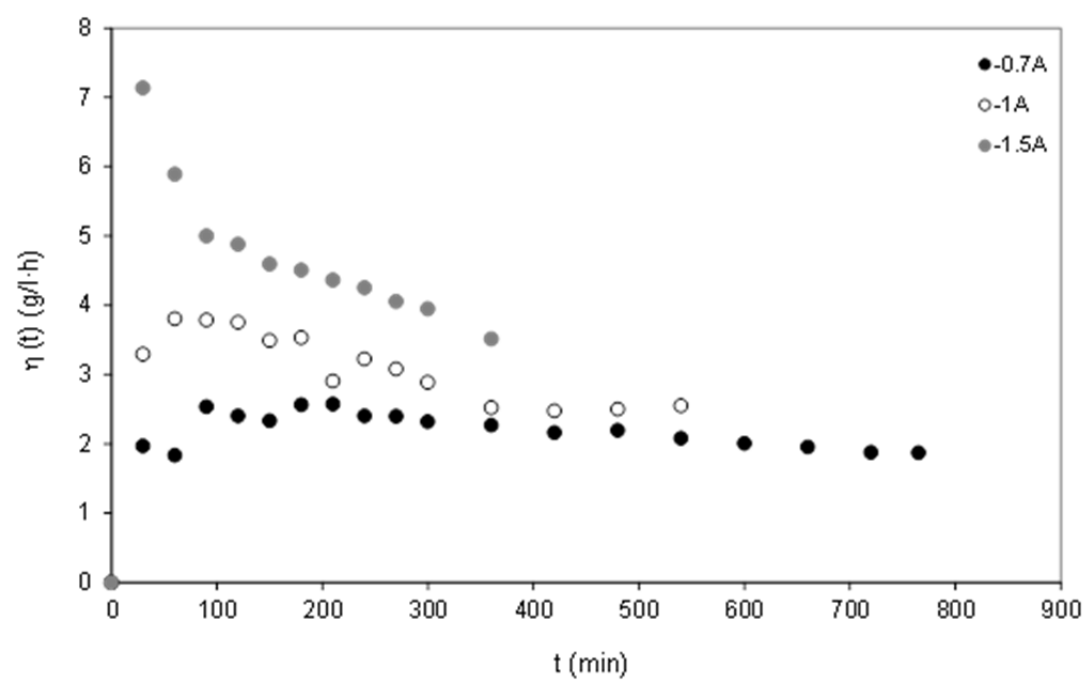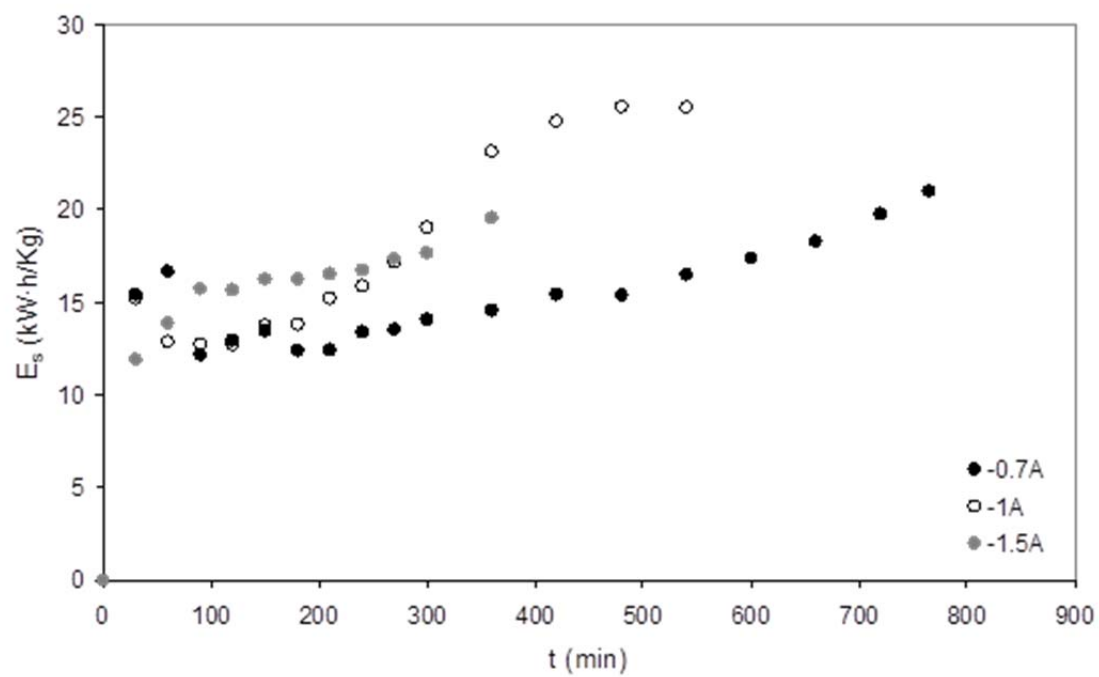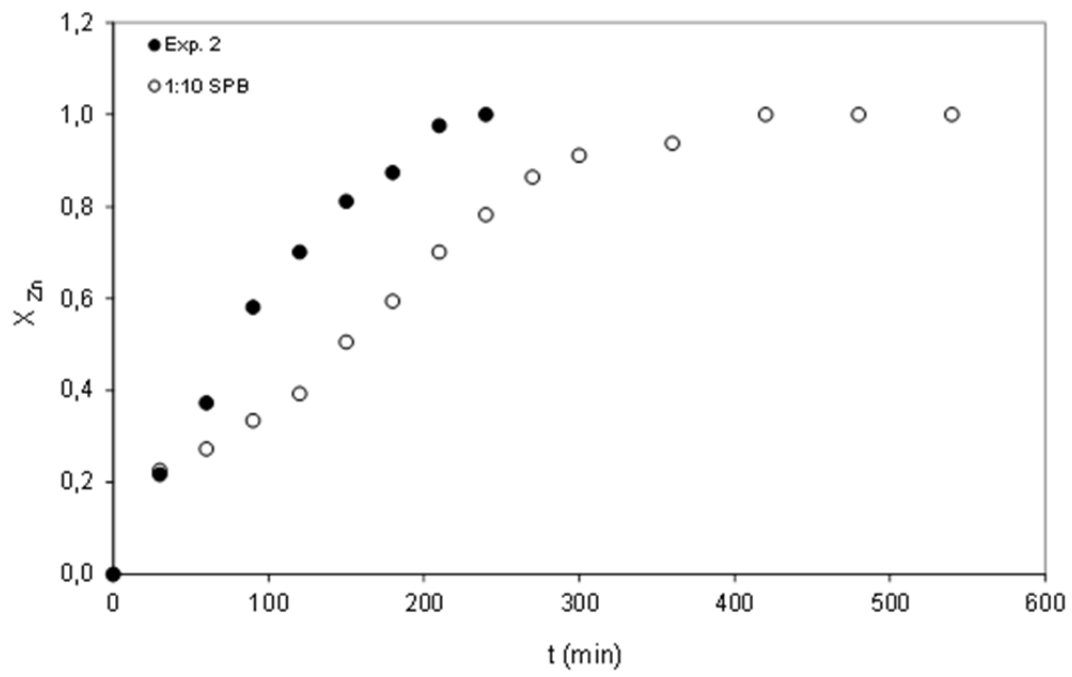
Figure 5
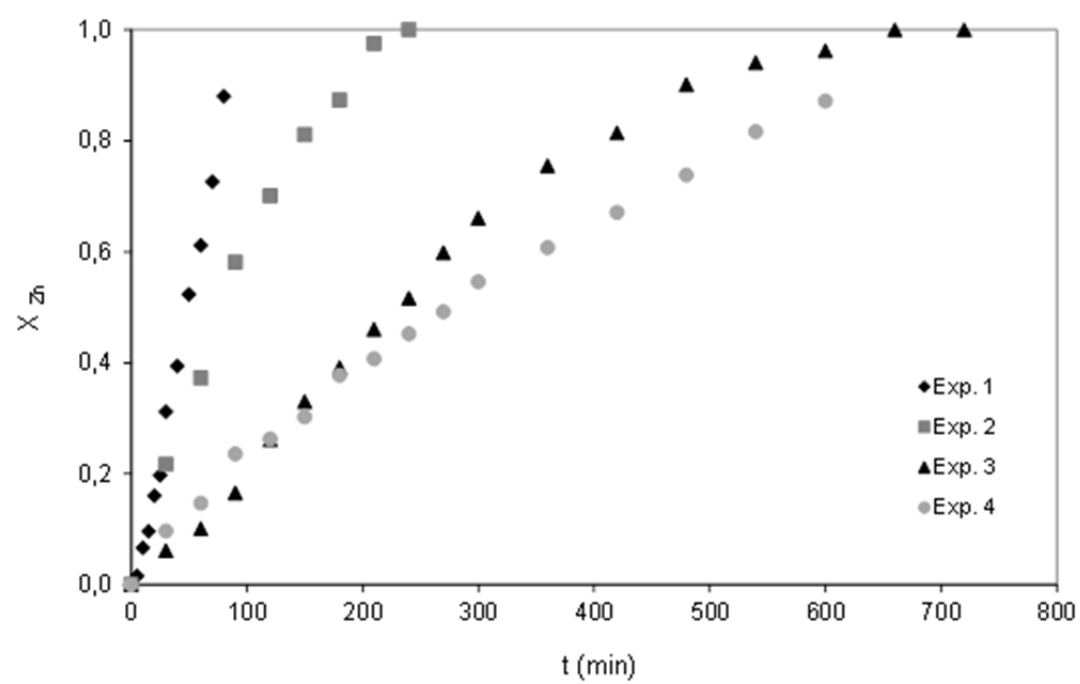
Figure 6
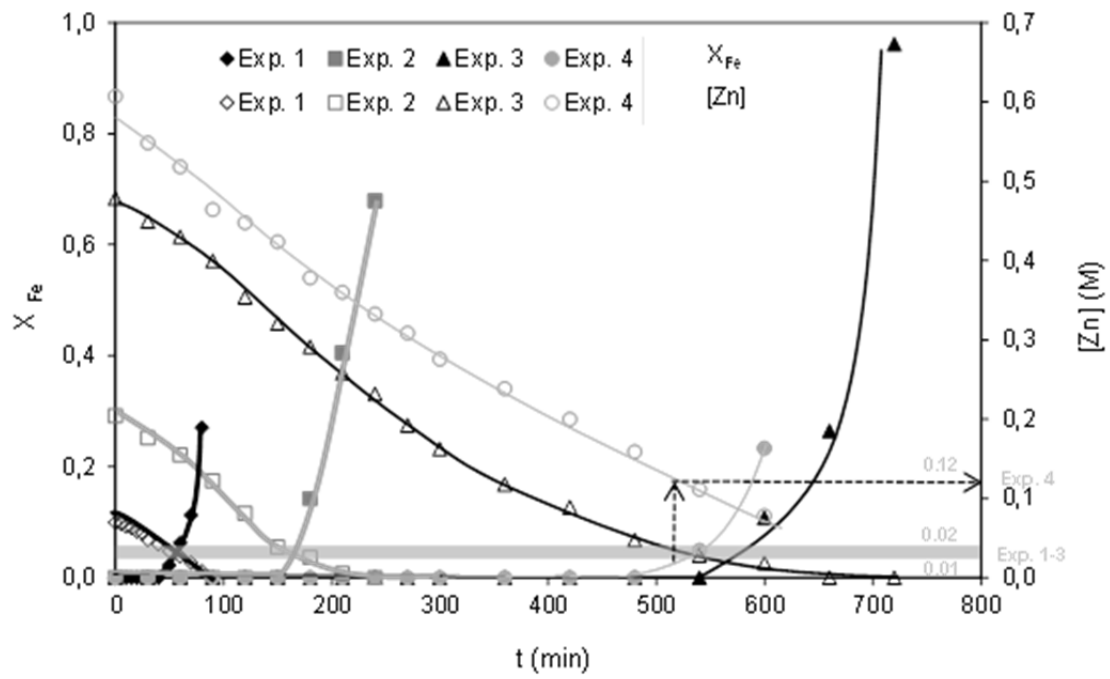
Figure 7
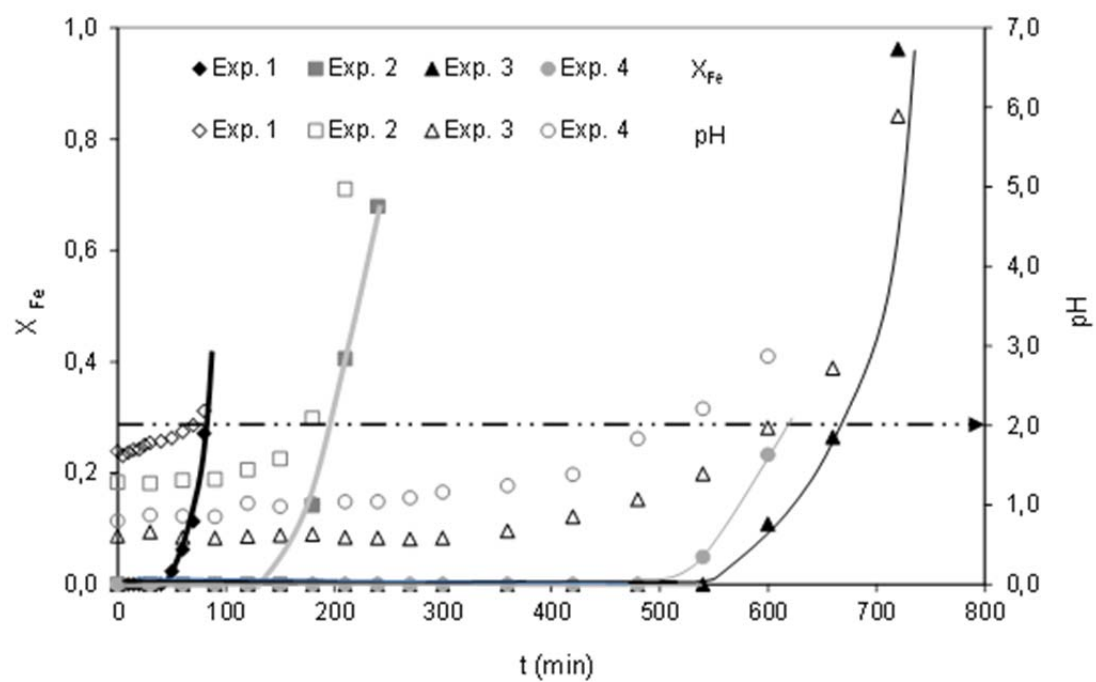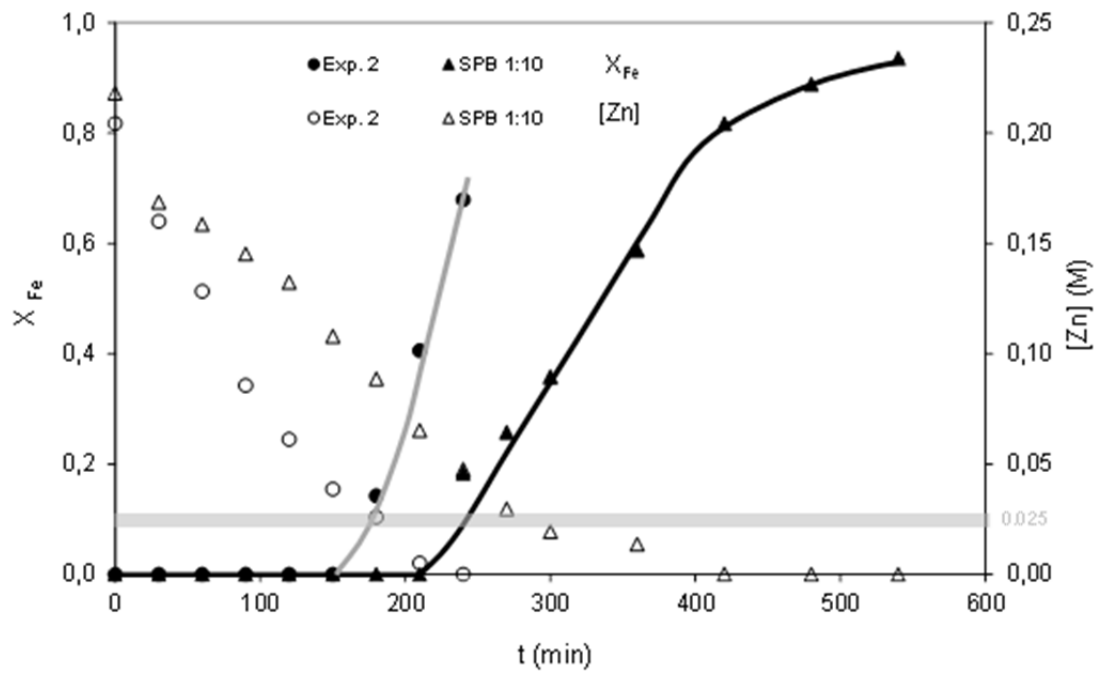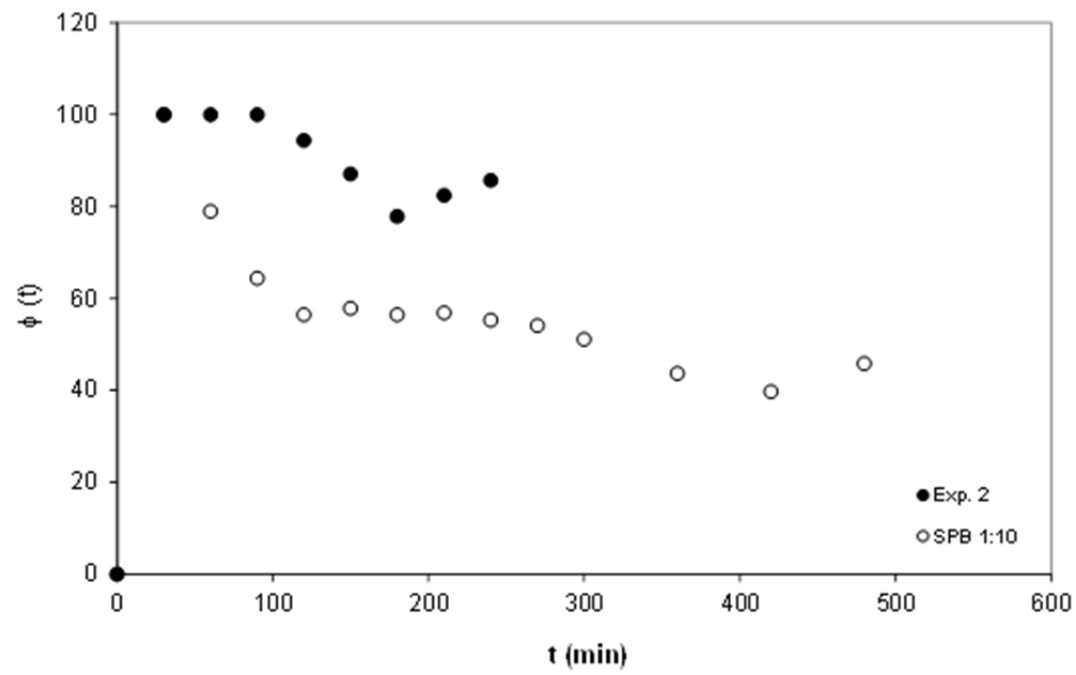
Figure 8

Figure 9

Figure 10

Figure 11

Figure 12

Figure 13

Figure 14

Figure 15

Figure 16
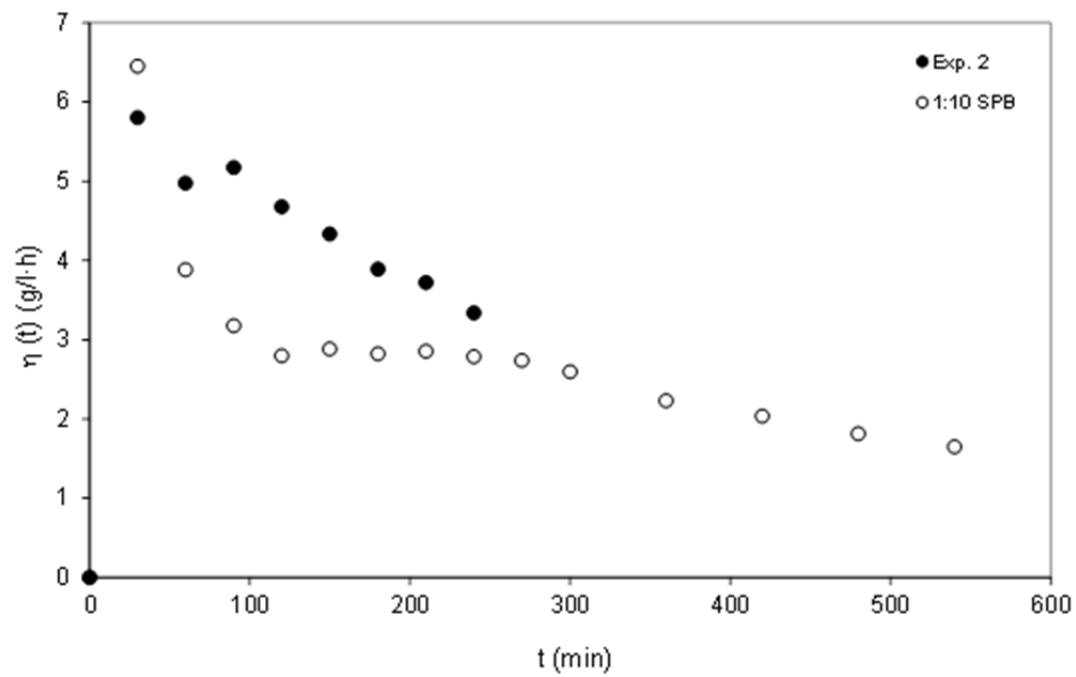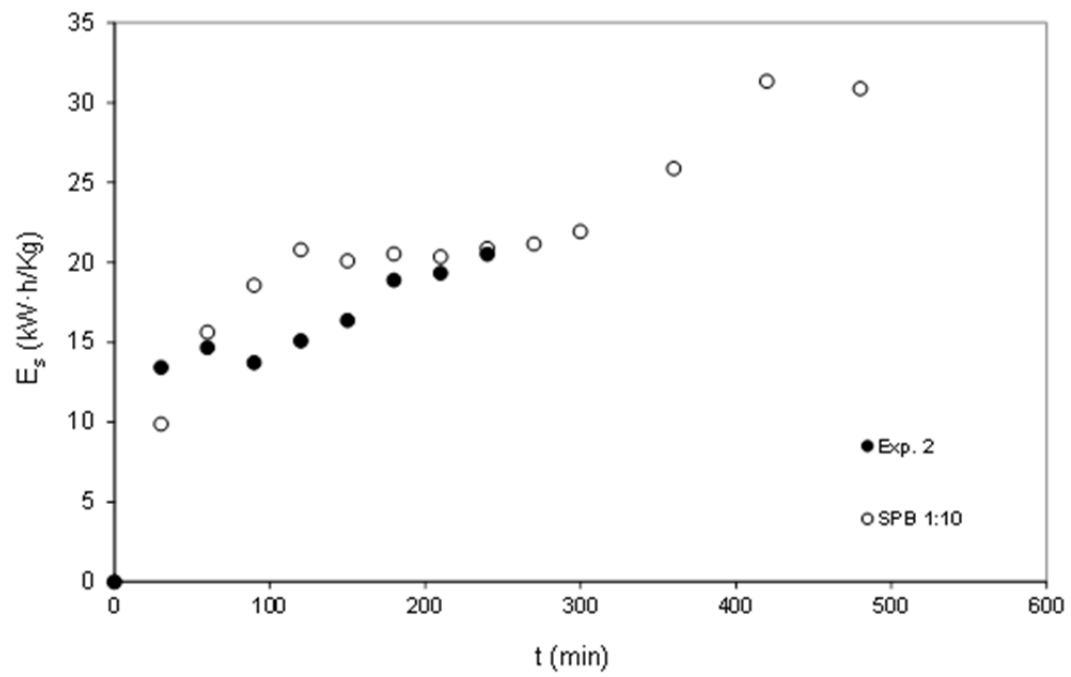
Figure 17

Figure 18

Table 1

Composition of real SPB.

Component	Concentration
$[H^+]$ (mol L^{-1})	1.10±0.04
$[Zn^{2+}]$ (mol L^{-1})	1.87±0.05
$[Fe]_{TOTAL}$ (g L^{-1})	1.70±0.05
$[Fe^{2+}]$ (g L^{-1})	1.66±0.04
$[Fe^{3+}]$ (g L^{-1})	0.04±0.03
$[Cl^-]$ (g L^{-1})	8.48±0.08

Table 2

Experimental conditions of EPT and EW experiments.

Exp.	Operation conditions			Stripping solution			
	EPT		EW				
	TBP (%v/v)	Operation time (h)	Applied current (A)	$[Zn^{+2}]$ (M)	$[Fe^{+2}]$ (M)	pH	$[Zn^{+2}]/[Fe^{+2}]$
1	20	1	-1.00	0.07	0.005	1.67	14.0
2		2		0.20	0.010	1.28	20.0
3		3		0.48	0.026	0.61	18.5
4	50			0.61	0.040	0.80	15.3
5[*]		1.5	-0.70	0.43	0.149	0.73	2.90
6[*]				0.45	0.085	0.79	5.30
7[*]				0.42	0.042	0.74	10.0
8				0.39	0.012	0.63	32.5
9			-1.00	0.40	0.019	0.89	21.1
10			-1.50	0.37	0.017	0.60	21.8

*Stripping solutions doped with $FeCl_2$ to modify the molar ratio zinc/iron

Table 3

Initial molar fractions of zinc chlorocomplexes in the stripping solutions employed in

EW experiments 3 and 4.

	Experiment 3	Experiment 4
$[Zn^{+2}]$ (M)	0.48	0.61
$[Cl^-]$ (M)	0.93	2.16
pH	0.61	0.80
Chlorocomplexes	Molar fraction	
$ZnCl_4^{-2}$	0.0461	0.265
$ZnCl_3^-$	0.0392	0.105
Zn^{+2}	0.71	0.405
$ZnCl_2$	0.0507	0.086
$ZnCl^+$	0.154	0.139